October 2022

GUIDANCE, NAVIGATION AND CONTROL FOR THE AUTONOMOUS RENDEZVOUS WITH AN UNCOOPERATIVE TUMBLING TARGET

A. Martinez, J. Ramirez, F. Cacciatore

ESA Clean Space Industry Days 22, ESTEC

Introduction | Study framework

Applications of in-orbit servicing

- ISS servicing (crew + cargo)
- In-orbit inspection, maintenance and refueling*
- Interplanetary exploration*
- Active Debris Removal (ADR)*
- …

***Autonomous AOCS/GNC is a key technology enabler**

Challenging scenario for GNC: ADR

- Target **uncooperativeness**
- Target is often in a **tumbling** state
- Ground estimates of the target state are subject to high uncertainty
- Relative dynamics not compatible with operation via telecommand (even in LEO)

Autonomous rendezvous and capture is required

Notice that the GNC technology developed for this study case can be applied to other cooperative and uncooperative rendezvous and capture scenarios with little tuning required.

Introduction | Study framework

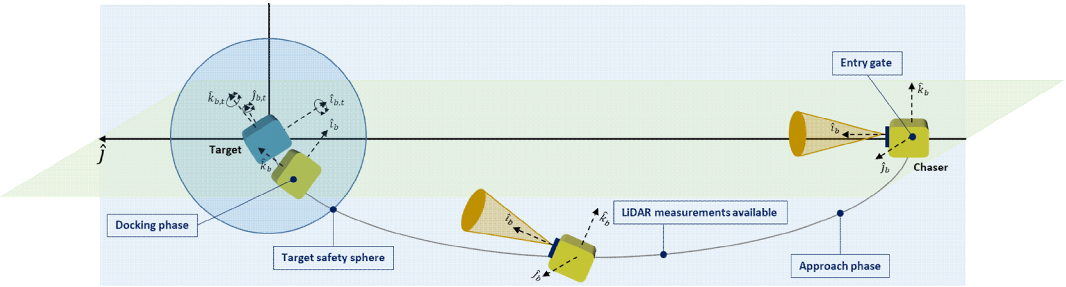

Objectives of the study

Autonomous rendezvous GNC technology development, applied to a generic LEO RVD study case with an uncooperative tumbling target:

- Optimal offline guidance, including FoV management and attitude synchronization
- Autonomous optical navigation
- Absolute and relative state estimation
- Classical and novel 6 dof control methodologies

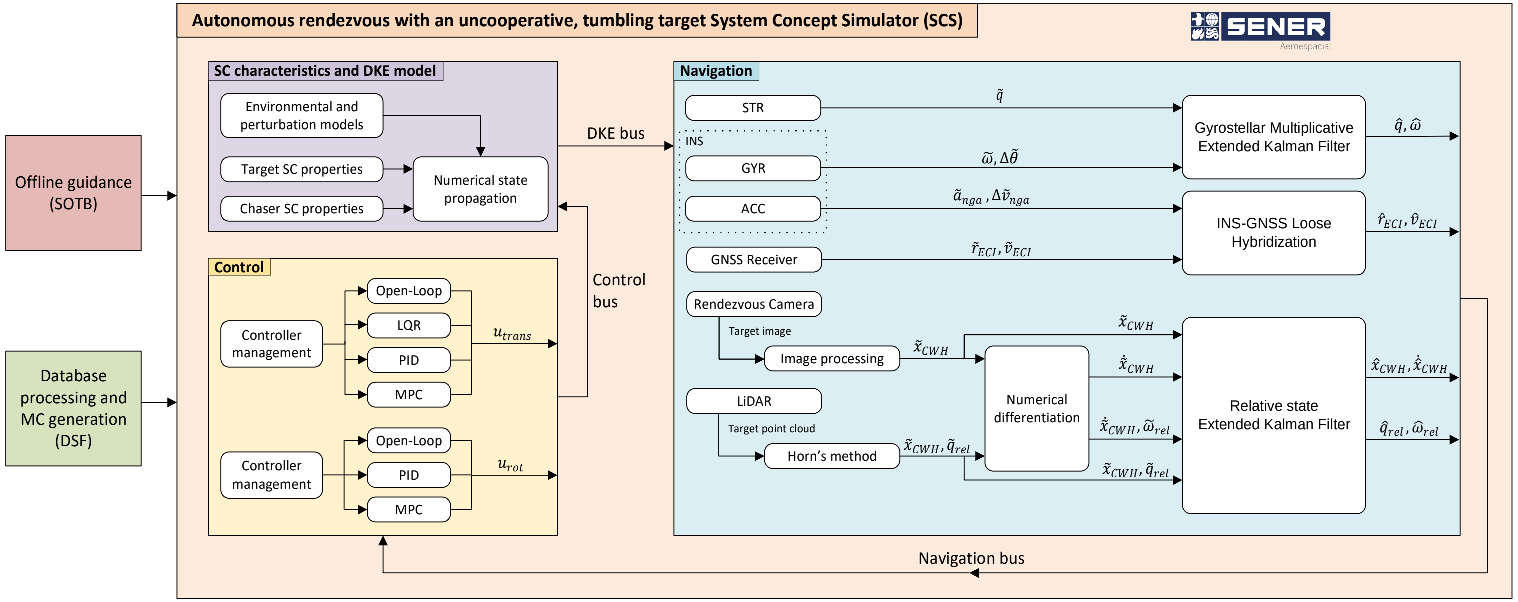

SENER Rendezvous Tool (**SERVO**)

- ✓ MATLAB/Simulink SCS for GNC technology development
- ✓ High fidelity environment simulation module embedded
- ✓ Controller alternatives evaluation
- ✓ Both the GNC and the SCS can be adapted and particularized to the required RVD scenario

Introduction | SENER Optimization Toolbox

SENER Optimization Tool Box

- ✓ **Optimization core for SERVO**
- ✓ In-house developed optimization suite
- ✓ Autocodable MATLAB implementation

- ✓ Interior point quadratic programming solver
- ✓ Dedicated solver for linear Model Predictive Control
- ✓ Sequential convex and quadratic programming extension

- ✓ Aimed for onboard implementation
- ✓ Focused on optimal guidance and control

Interface for optimal control:

$$
\begin{aligned}
\min_{x_i \in \mathbb{R}^{n_x}, u_i \in \mathbb{R}^{n_u}, \gamma \in \mathbb{R}^{n_s}} \quad & \frac{1}{2} x_N^T P x_N + p^T x_N + \frac{1}{2}\gamma^T C \gamma + c^T \gamma + \sum_{i=0}^{N-1} \frac{1}{2} x_i^T L_i x_i + l_i^T x_i + \frac{1}{2} u_i^T R_i u_i + r_i^T u_i \\
\text{s.t.} \quad & x_{i+1} = f_i(x_i, u_i); \quad \forall i = 0, .., N-1, \\
& A_i^x x_i \leq b_i^x + J_i^{\text{aff},x} \gamma; \quad \forall i = 1, ..., N, \\
& A_i^u u_i \leq b_i^u + J_i^{\text{aff},u} \gamma; \quad \forall i = 0, ..., N-1, \\
& \frac{1}{2} x_i^T Q_{i,j}^x x_i + (q_{i,j}^x)^T x_i \leq c_{i,j}^x + (J_{i,j}^{q,x})^T \gamma; \quad \forall j = 1, ..., n_{xi}^q; \forall i = 1, ..., N, \\
& \frac{1}{2} u_i^T Q_{i,j}^u u_i + (q_{i,j}^u)^T u_i \leq c_{i,j}^u + (J_{i,j}^{q,u})^T \gamma; \quad \forall j = 1, ..., n_{ui}^q; \forall i = 0, ..., N-1, \\
& \gamma \geq 0, \\
& x_0 = x_{\text{init}}
\end{aligned}
$$

Competitive performance:

Table 1: Benchmark QP performance comparison of SOTB against @quadprog

QP size	SOTB QCQP		@quadprog	
(# variables | # constraints)	Median # iterations	Mean solve time [s]	Median # iterations	Mean solve time [s]
2 | 4	5	0.002	4	0.003
256 | 1154	20	0.143	22	0.662
240 | 480	8	0.092	6	0.006
20 | 80	9	0.010	8	0.003
60 | 630	117	0.438	*Not solved*	*Not solved*
75 | 470	37	0.154	*Not solved*	*Not solved*
57 | 434	35	0.120	*Not solved*	*Not solved*

Guidance | Trajectory guidance problem

- **Dynamic model:** Clohessy-Wiltshire-Hill (CWH) equations. Valid for:
  - Small eccentricity orbits
  - Close target-chaser manoeuvering
  - First-order approximation of the gravitational field

$$\begin{cases} \ddot{x} - 2n\dot{y} - 3n^2 x = a_x = f_x/m \\ \ddot{y} + 2n\dot{x} = a_y = f_y/m \\ \ddot{z} + n^2 z = a_z = f_z/m \end{cases}$$

Clohessy-Wiltshire-Hill (CWH) equations

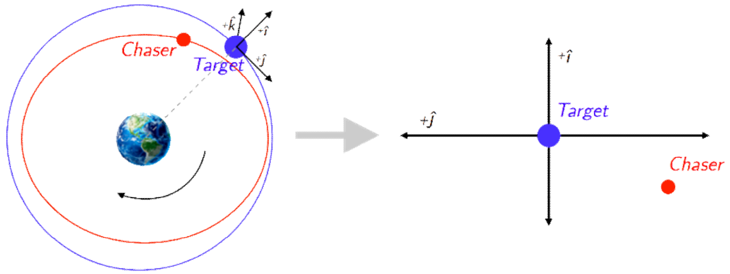

Hill's reference frame

- **Optimal control problem:** end-state matching

$$f_i(x_i, u_i) = A_d x_i + B_d u_i/m$$

$$\begin{aligned} \min_{x_i, u_i, \gamma} \quad & \frac{1}{2}\left(x_N - x_{ref_N}\right)^T P \left(x_N - x_{ref_N}\right) + \sum_{i=0}^{N-1} \frac{1}{2} u_i^T R_i u_i \\ \text{s.t.} \quad & x_{i+1} = f_i\left(x_i, u_i\right); \qquad \forall i = 0, \ldots, N-1 \\ & |u_i| \le u_{max}; \qquad \forall i = 0, \ldots, N-1 \\ & x_0 = x_{\text{init}} \end{aligned}$$

with

$$x_{ref_N} = [x_f, y_f, z_f, \dot{x}_f, \dot{y}_f, \dot{z}_f]^T \qquad u_{max} = I_{3,1} F_{max}$$

$$x_{\text{init}} = [x_0, y_0, z_0, \dot{x}_0, \dot{y}_0, \dot{z}_0]^T$$

- **Total maneuver time:** 3,000 seconds
- **Total maneuver cost:** $\Delta v_{tot} = 2.11$ m/s

using V-bar guidance…

N_{burn} $[-]$	4	6	8	10	20	30	40	$\boxed{44}$
Δv_{tot} $[m/s]$	5.79	5.03	4.50	4.11	3.04	2.52	2.21	$\boxed{2.11}$

V-bar classical guidance cost as a function of the number of burns

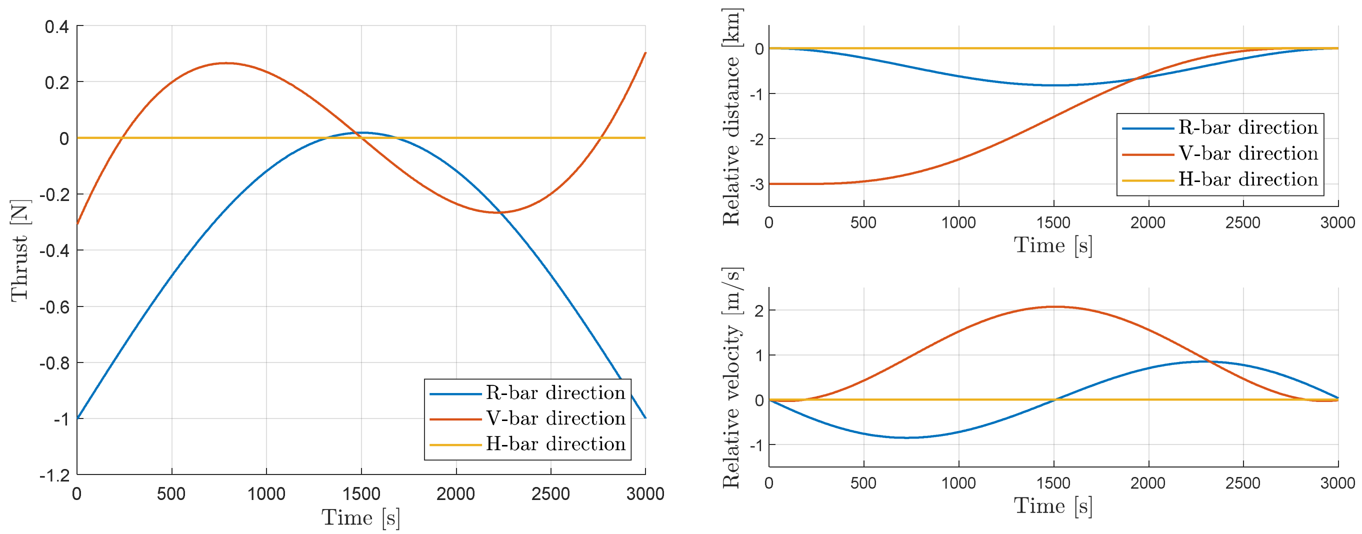

Optimal control profile and associated translational trajectory in CWH frame

Guidance | Attitude guidance for the approach phase: Line-of-Sight management

- **Dynamic model:** chaser absolute rotational state kinematics and dynamics

$$\begin{cases} \dot{\vec{q}}_{bi} = \frac{1}{2}\vec{\omega}_b^{bi} \otimes \vec{q}_{bi} \\ \dot{\vec{\omega}}_b^{bi} = \left(\bar{\bar{J}}_b^c\right)^{-1}\left[\vec{L}_b^c - \vec{\omega}_b^{bi} \times \left(\bar{\bar{J}}_b^c \vec{\omega}_b^{bi}\right)\right] \end{cases}$$

- **Reference attitude quaternion generation for LoS:**

Relative position vector

Instrument boresight

$$\cos\theta = \vec{r}\cdot\vec{\nu}\,,\ \hat{e} = \vec{r}\times\vec{\nu}/|\vec{r}\times\vec{\nu}|$$

$$\vec{q}_{rv} = [\hat{e}\sin(\theta/2), \cos(\theta/2)]^T$$

$$\vec{q}_k = \vec{q}_{k-1} \otimes \vec{q}_{rv}$$

- **Optimal control problem:** path tracking (for attitude quaternion)

$$\min_{x_i, u_i, \gamma} \quad \frac{1}{2}\left(x_N^q - x_{ref_N}^q\right)^T P\left(x_N^q - x_{ref_N}^q\right) + \frac{1}{2}\sum_{i=0}^{N-1}\left[\left(x_i^q - x_{ref_i}^q\right)^T L_i\left(x_i^q - x_{ref_i}^q\right) + u_i^T R_i u_i\right]$$

$$\begin{aligned} \text{s.t.} \quad & x_{i+1} = f_i(x_i, u_i)\,; && \forall i = 0, \ldots, N-1 \\ & |u_i| \le u_{max}; && \forall i = 0, \ldots, N-1 \\ & x_0 = x_{\text{init}} \end{aligned}$$

with

$$x_{\text{init}} = [q_0, \omega_0]^T$$

$$x_{ref_N}^q = q_{ref_N} \qquad u_{max} = I_{3,1}T_{max}$$

Note: non-linear dynamic model

$$\dot{x} = g(x,u) = [\dot{q}_{bi}, \dot{\omega}_b^{bi}]^T = A(x,u)x + B(x,u)u$$

with

$$A = \partial g(x,u)/\partial x\,,\ B = \partial g(x,u)/\partial u$$

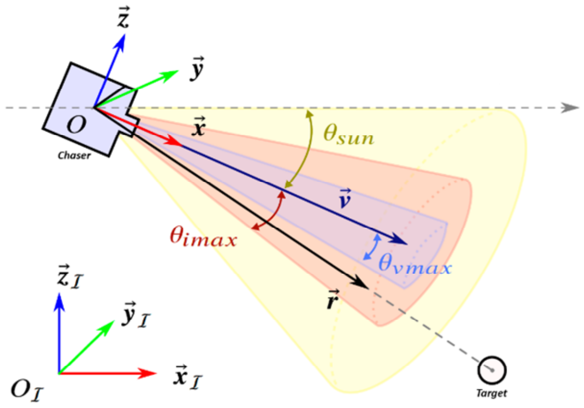

LoS management problem definition

V. Preda, A. Hyslop and S. Bennani. "Optimal Science-time Reorientation Policy for the Comet Interceptor Flyby via Sequential Convex Programming". In *CEAS Space Journal* (Apr. 2021).

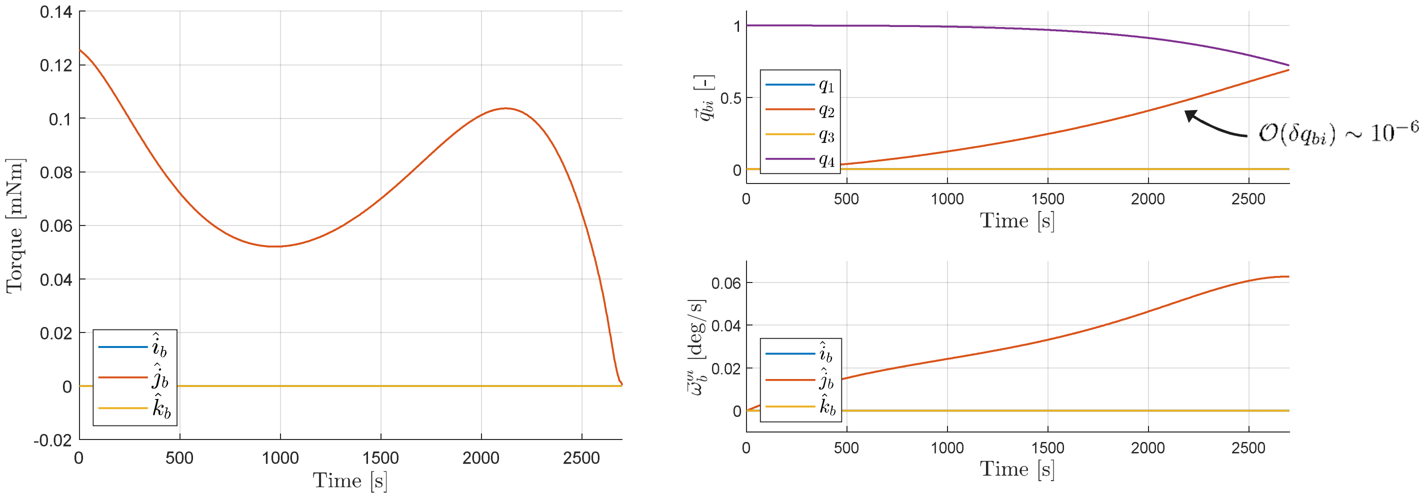

Optimal control profile and associated rotational chaser state (approach)

Guidance | Attitude guidance for the capture phase: Attitude synchronization

- **Dynamic model:** chaser-target relative rotational state kinematics and dynamics

$$\begin{cases} \dot{\vec{q}} = \frac{1}{2}\vec{\omega} \otimes \vec{q} \\ \dot{\vec{\omega}} = \left(\bar{\bar{J}}_c\right)^{-1}\left[\vec{L}_b^c - \left[\vec{\omega} + C_{c/t}\vec{\omega}_t\right]^{\times} \bar{\bar{J}}_c\left(\vec{\omega} + C_{c/t}\vec{\omega}_t\right)\right] - C_{c/t}\left[\bar{\bar{J}}_t^{-1}\left(-\left[\vec{\omega}_t\right]^{\times} \bar{\bar{J}}_t\vec{\omega}_t\right)\right] - \left[C_{c/t}\vec{\omega}_t\right]^{\times}\vec{\omega} \end{cases}$$

- **Optimal control problem:** end-state matching

$$\begin{aligned} \min_{x_i, u_i, \gamma} \quad & \frac{1}{2}\left(x_N - x_{ref_N}\right)^T P \left(x_N - x_{ref_N}\right) + \sum_{i=0}^{N-1} \frac{1}{2} u_i^T R_i u_i \\ \text{s.t.} \quad & x_{i+1} = f_i\left(x_i, u_i\right); \quad \forall i = 0, \ldots, N-1 \\ & A_i^u u_i \le b_i^u; \quad \forall i = 0, \ldots, N-1 \\ & x_0 = x_{\text{init}} \end{aligned}$$

with

$$x_{ref_N} = [0,0,0,1,0,0,0]^T \qquad x_{\text{init}} = [q_{N,app}, \omega_{N,app}]^T$$

$$A_i^u = [I_{1,3}, -I_{1,3}] \qquad b_i^u = u_{max} I_{3,1}$$

$$\vec{q}_{N,app} = \vec{q}^{\,c}_{N,app} \otimes \vec{q}^{\,t*}_{N,app}\,, \quad \vec{\omega}_{N,app} = C_{c/t}\vec{\omega}^{\,t}_{N,app} - \vec{\omega}^{\,c}_{N,app}$$

Note: non-linear dynamic model

$$\dot{x} = g(x,u) = [\dot{q}_{bi}, \dot{\omega}_b^{bi}]^T = A(x,u)x + B(x,u)u$$

with

$$A = \partial g(x,u)/\partial x\,,\; B = \partial g(x,u)/\partial u$$

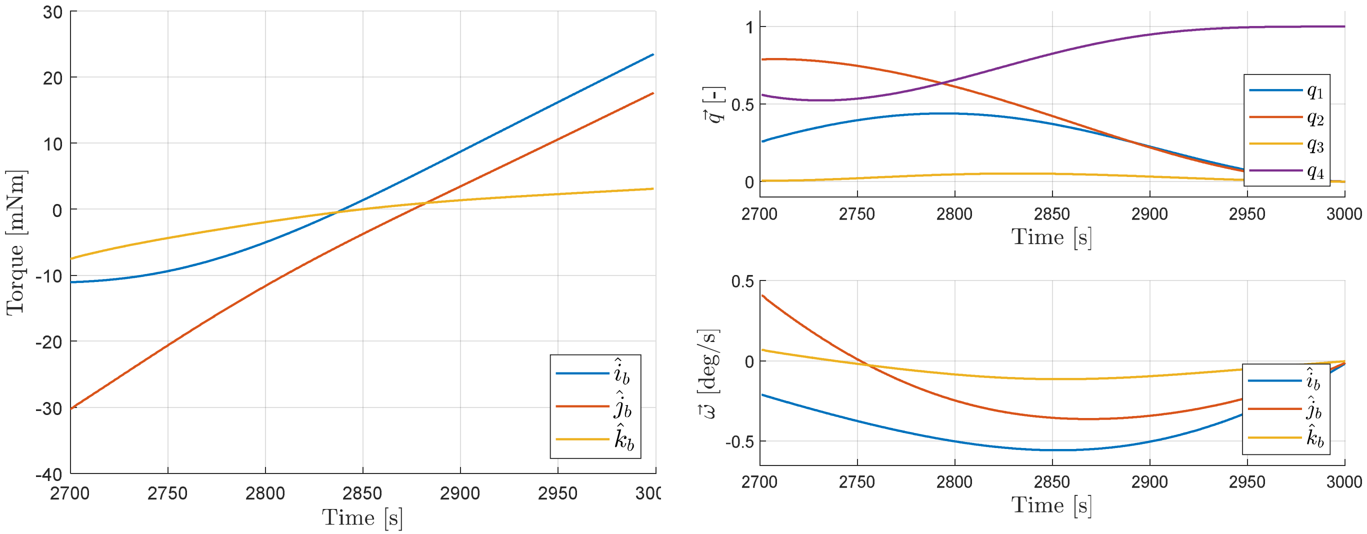

Optimal control profile and associated relative rotational state (capture)

Navigation | Measurement model

Relative state measurement

- **Rendezvous Camera** reflector images processing logic:

Compute the number of pixels illuminated
Image histogram analysis

Compute the Center of Brightness (CoB)

$$\tilde{x}_{\mathrm{f_p}} = \frac{\sum_i \sum_j x_i I_{v_{ij}}}{\sum_i \sum_j I_{v_{ij}}} \quad \tilde{y}_{\mathrm{f_p}} = \frac{\sum_i \sum_j y_j I_{v_{ij}}}{\sum_i \sum_j I_{v_{ij}}}$$

Compute the relative camera-reflector distance

$$\tilde{d} = \frac{L_{side} \times f}{\tilde{n}_{px} \times d_{px}}$$

Compute the reflector azimuth and elevation

$$\tilde{\theta} = \theta_{\max} \frac{\tilde{x}_{\mathrm{f_p}}}{x_{\max}} \quad \tilde{\phi} = \phi_{\max} \frac{\tilde{y}_{\mathrm{f_p}}}{y_{\max}}$$

Compute the relative position vector

$$\begin{cases} \tilde{x}_{\mathrm{t/RVC}} = \tilde{d}\cos(\tilde{\phi})\cos(\tilde{\theta}) \\ \tilde{y}_{\mathrm{t/RVC}} = \tilde{d}\cos(\tilde{\phi})\sin(\tilde{\theta}) \\ \tilde{z}_{\mathrm{t/RVC}} = \tilde{d}\sin(\tilde{\phi}) \end{cases}$$

Compute the relative velocity vector
Least Squares Polynomial Fitting differentiation

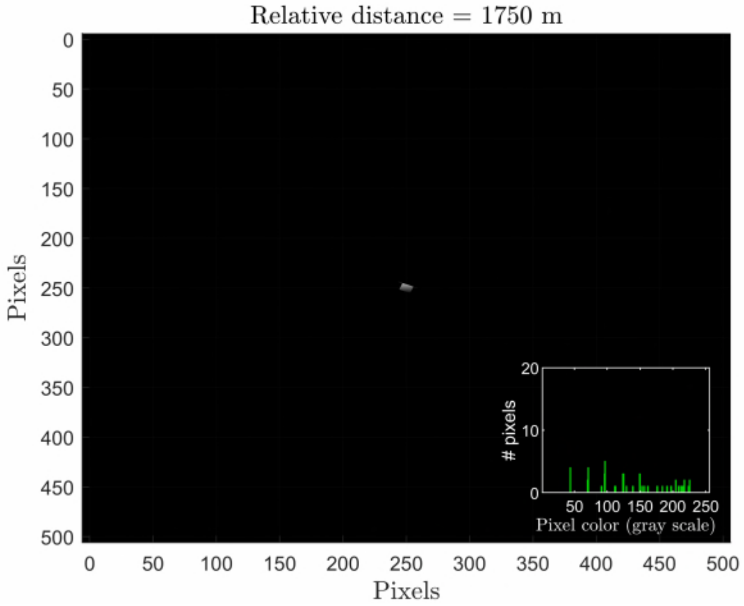

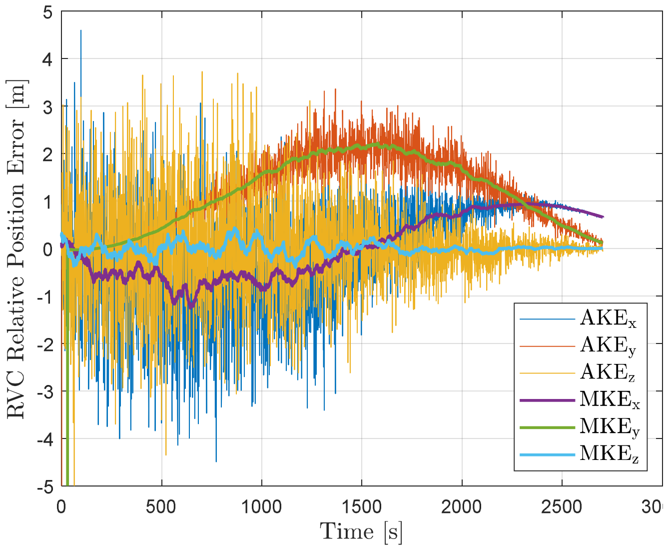

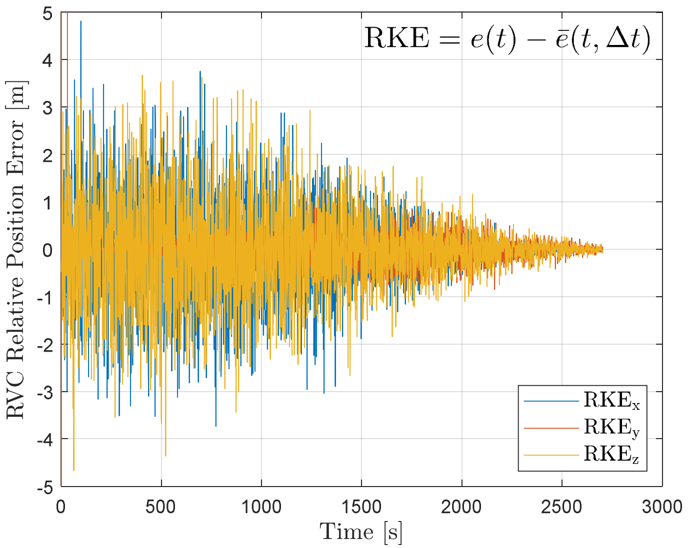

RVC Relative Position AKE, MKE and RKE

Navigation | Measurement model

Relative state measurement

- **3D LiDAR** target point cloud processing logic:
  - **Measurement error metric:** Hausdorff distance

$$d_{\mathrm{H}}(X,Y) = \max\left\{\sup_{x\in X} d(x,Y), \sup_{y\in Y} d(X,y)\right\}$$

Greatest of all the distances from a point in one set to its nearest neighbour in the other set.

  - **Pose reconstruction:** Horn's method (quaternion-based)

$$\min \sum_{i=1}^{n} ||e_i||^2 = \sum_{i=1}^{n} ||r_{r,i} - sRr_{l,i} - r_0||^2$$

This is the general formulation of the ICP methodology. Horn's method solves an eigenvalue-eigenvector problem to find the best orthonormal fit.

  - **Relative velocity and angular velocity:** Least Squares Polynomial Fitting differentiation

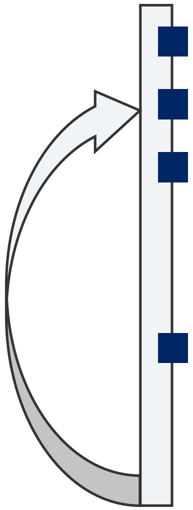

- Initialize the buffer
- Fill the buffer with the sensor measurements
- Fit an n order polynomial

  $p(x) \leftarrow V^{-1}y$ Vandermonde's matrix

  where

  $p(x) = p_1x^n + p_2x^{n-1} + \cdots + p_nx + p_{n+1}$
- Evaluate the derivative of the measurement

  $dy \leftarrow dx(x = y)$

  where

  $dp(x) = p_1nx^{n-1} + p_2(n-1)x^{n-2} + \cdots + p_n$

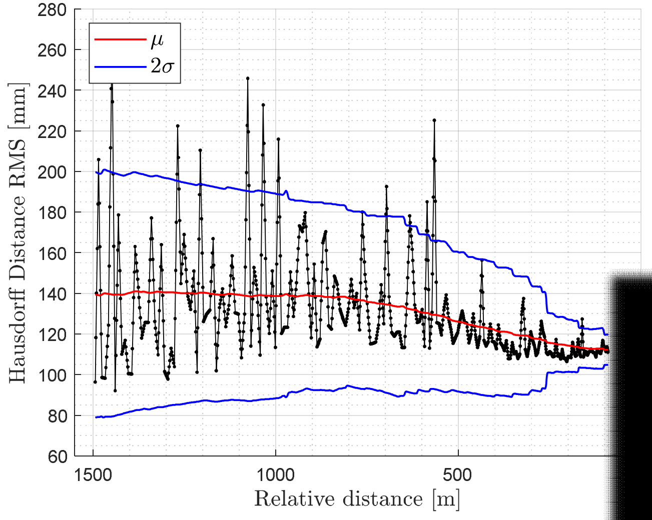

Hausdorff Distance RMS vs relative distance

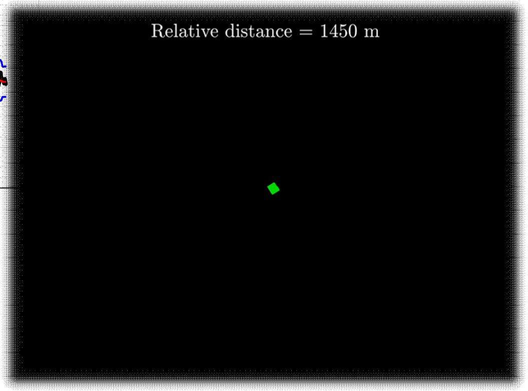

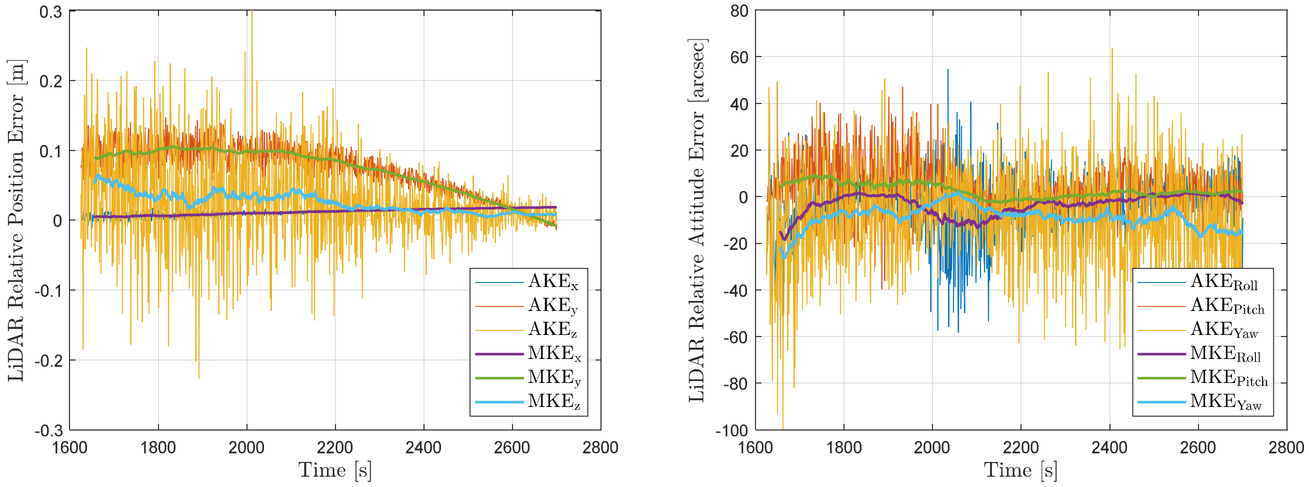

RVC Relative Position and Attitude AKE and MKE

Gyrostellar Multiplicative Extended Kalman Filter

- **Objective:** fuse GYR integrated angle (high frequency, but subject to drift), with the STR attitude quaternion (low frequency) ⟶ unbiased attitude estimation

INS-GNSS Loose Hybridization

- **Objective:** fuse the ACC integrated position and velocity (high frequency, but subject to drift), with the GNSS processed position and velocity solution (low frequency) ⟶ unbiased position and velocity estimation

Relative state Extended Kalman Filter

- **Objective:** fuse the Rendezvous Camera (RVC) and LiDAR measurements ⟶ chaser-target pose estimation
- **Multisensor, multirate Extended Kalman Filter,** with a sequential architecture

Propagate state and covariance matrix. Update relative attitude quaternion.

$$\hat{x}_k^- \leftarrow f(\hat{x}_{k-1}^+, u_k)\,,\ \hat{q}_{rel,k}^- \leftarrow \hat{q}_{rel,k-1}^+ \odot q(\Delta\phi_{rel,k}^-) \quad P_k^- \leftarrow F_k P_{k-1}^+ F_k^T + Q_k$$

Sequentially for the RVC and LiDAR measurements

Compute Kalman gain

$$K_k \leftarrow P_k^- H_k^T (H_k P_k^- H_k^T + R_k)^{-1}$$

Update delta-state with RVC/LiDAR measurement

$$\Delta x_k^+ \leftarrow \Delta x_k^- + K_k (z_k - H_k \Delta x_k^-),\ \text{with}\ \Delta x_k^- \equiv 0\,,\ z_k = y_k - h(\hat{x}_k^-)$$

Full state reset

$$\hat{x}_k^+ = \hat{x}_k^- + \Delta\hat{x}_k^+\ \text{, except}\ \hat{q}_{rel,k}^+ = \hat{q}_{rel,k}^- \odot \delta q(\delta\phi_{rel,k}^+)$$

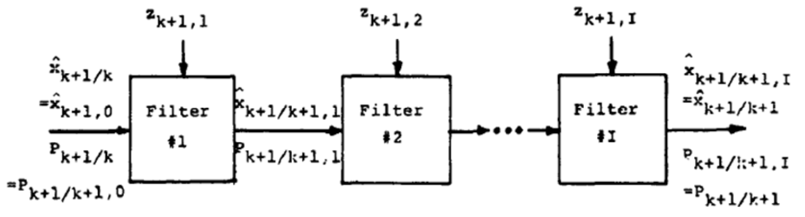

Sequential architecture for multisensor, multirate KF

$$\hat{x}_k^- = f(\hat{x}_{k-1}^+, u_k) = \begin{cases} A_{\mathrm{CWH}}[\hat{x}_{\mathrm{CWH}}, \dot{\hat{x}}_{\mathrm{CWH}}]^T + B_{\mathrm{CWH}} u_{\mathrm{CWH}} \\ -\hat{\omega}_{rel} \times \hat{\phi}_{rel} \\ A_{\omega_{rel}} \hat{\omega}_{rel} + B_{\omega_{rel}} u_{\omega_{rel}} \end{cases}$$

Control | Control alternatives description

Linear Quadratic Regulator

- Optimal linear controller for **trajectory tracking**
- **Application limited to LTI controllable systems**
- **Tuning:** Bryson’s rule + step response analysis

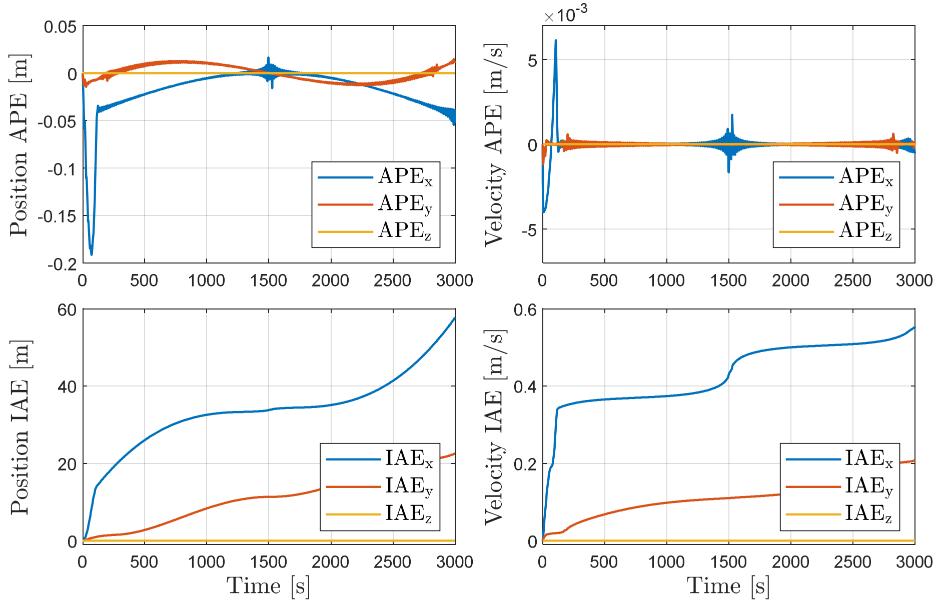

LQR translational state tracking APE and IAE

Performance error metrics: $\text{APE} = e_c(t) = x_{ref} - x \quad \text{IAE} = \int_0^t |e_c(t)|dt$

Proportional-Integral-Derivative Controller

- Widely used controller for **trajectory tracking**
- **Application:** linear and non-linear systems
- **Tuning:** Ziegler-Nichols method ($1/4$ wave decay) and response analysis

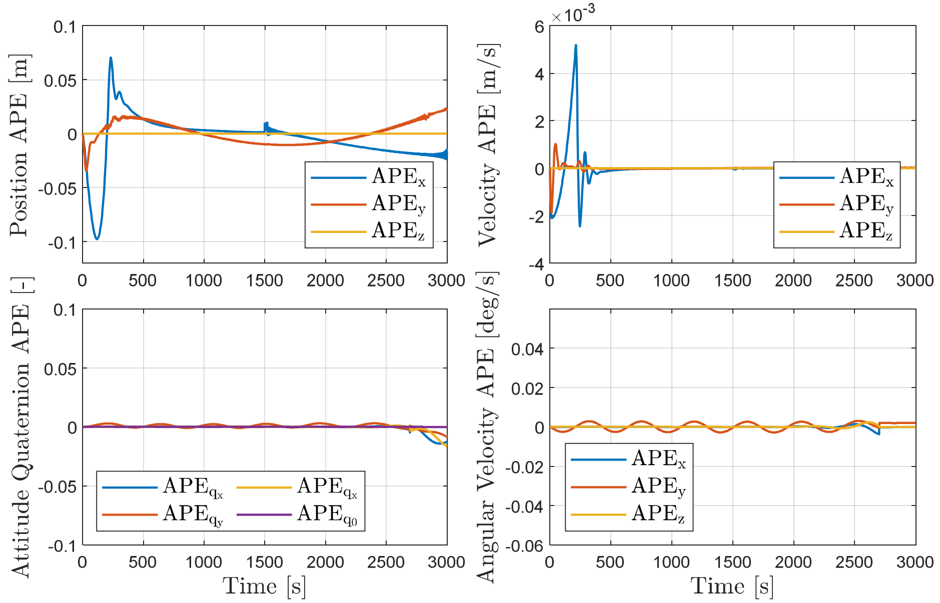

PID translational and rotational states tracking APE

Note: Both controllers operate with a 10 Hz control frequency

Control | Control alternatives description

Model Predictive Control scheme

- Based on a quasi-real time onboard solution of the optimal control problem with a **shrinking horizon**.
- It makes use of the current state of the system and a model for its future behaviour.
- **High robustness** and **nearly-optimal maneuver cost.**

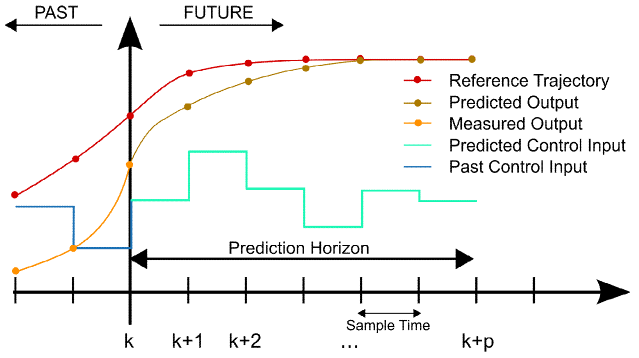

Shrinking horizon concept in Model Predictive Control

Relative translational state

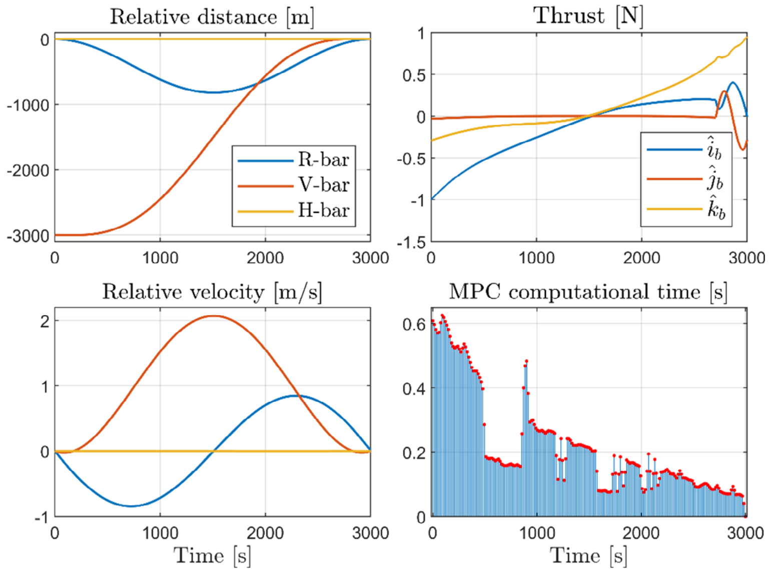

Chaser rotational state

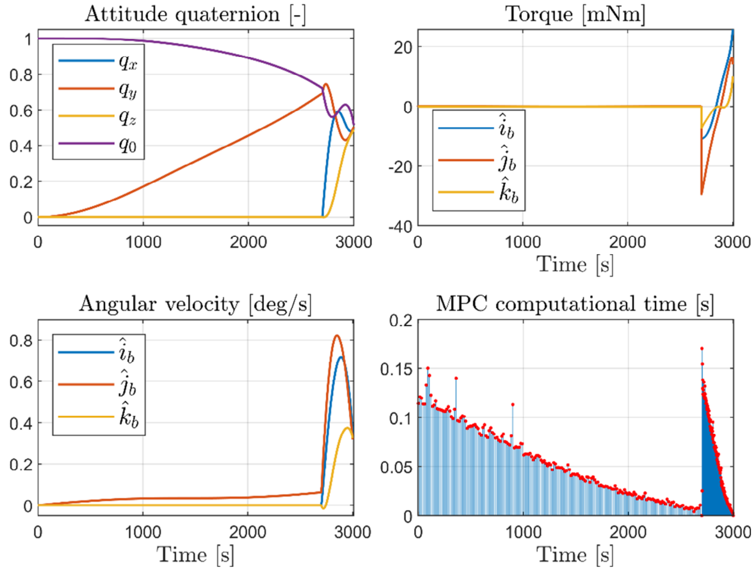

- **Reference case**: offline guidance
- **PID** controller tracking performance and end-state residual is aceptable, but its cost is highly sub-optimal.
- **MPC** provides a superior performance with respect to the other alternatives, at a nearly-optimal maneuver cost.
- It also provides greater flexibility in the design of the maneuver and incorporates actuation limitations in the problem formulation.

	Open Loop	LQR	PID	MPC
$\lvert\delta\vec{r}_f\rvert$ [cm]	1,066.88	5.37	3.11	0.60
$\lvert\delta\vec{v}_f\rvert$ [mm/s]	44.04	0.47	0.00	2.05
$\Delta v_{tot}/\Delta v_{tot,ref}$ [%]	N/A	+21.99	+21.71	+1.99
$[\delta\phi_f, \delta\theta_f, \delta\psi_f]$ [deg]	$[-5.14, 4.33, 2.81]$	N/A	$[1.43, 0.99, 1.90]$	$[0.35, 0.61, 0.39]$
$\delta\vec{\omega}_f$ [arcsec/s]	$[-88.565.28 - 8.30]$	N/A	$[-0.12, 7.06, -0.40]$	$[0.79, 3.89, 0.66]$

Control alternatives trade-off analysis results

SENER

Monte Carlo campaign

MPC controller response to initial relative state uncertainties

Analysis summary

- Perturbations:
  - Initial target attitude
  - Initial chaser-target pose
- Controller: MPC
- Confidence level: 99.73%
- Number of samples: 350

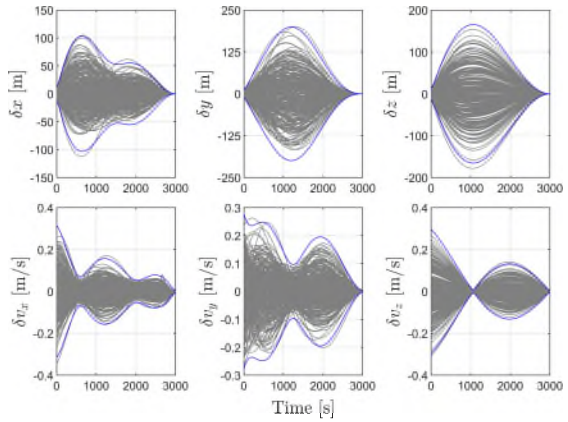

Translational state error and 3σ envelopes

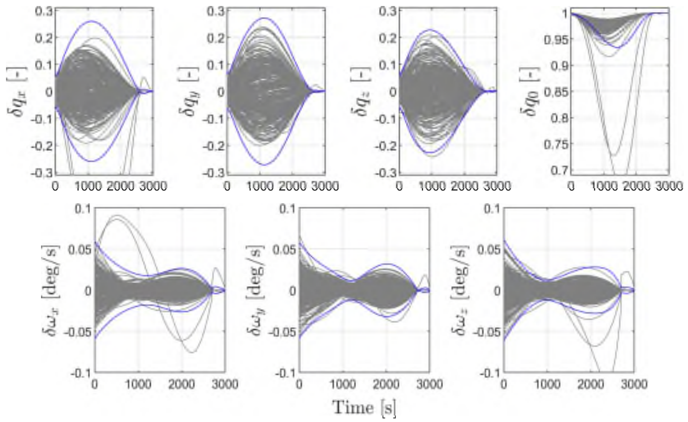

Rotational state error and 3σ envelopes

Data fusion algorithms response to navigation uncertainties

Analysis summary

- Perturbations:
  - GYR + ACC initial bias, SF and misalignments
  - GNSS receiver clock initial bias
  - GNSS non-deterministic environmental variables
  - Seeds of all stochastic processes
- Controller: MPC
- Confidence level: 99.73%
- Number of samples: 200

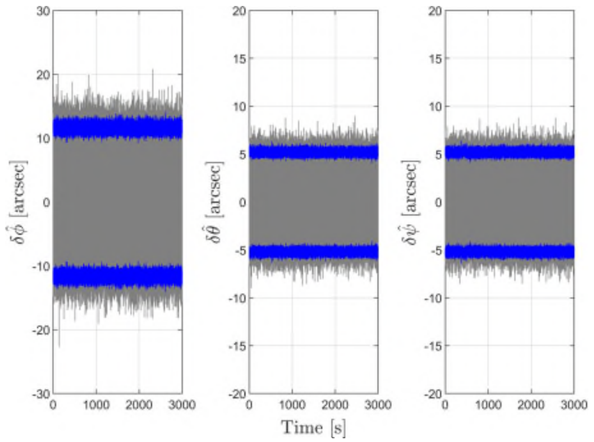

Gyrostellar chaser attitude knowledge error

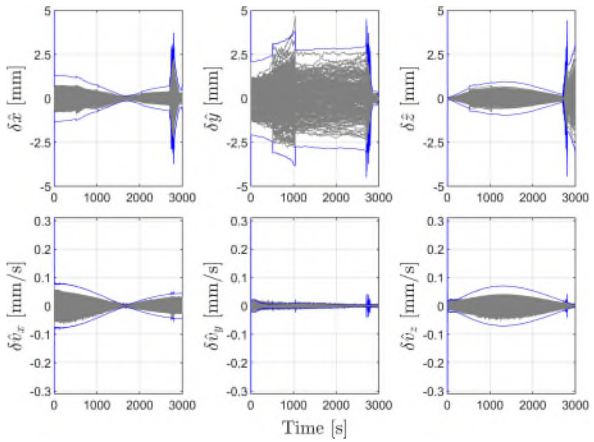

INSS-GNSS chaser PV knowledge error

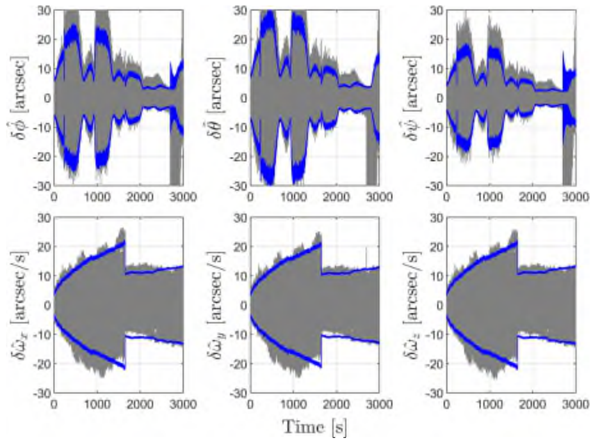

Chaser-target relative state knowledge error

Conclusions

Key contribution: complete autonomous AOCS/GNC loop for rendezvous and capture in high-uncertainty scenarios

- GNC solution enhanced with onboard convex optimization for guidance and control and optical navigation for an increased relative state knowledge.
- Demonstrated increase in operational flexibility, efficiency and robustness with respect to classical approaches.
- Technological contribution implemented in a high-fidelity System Concept Simulator, including synthetic Rendezvous Camera images and 3D LiDAR point cloud generation.
- Relative navigation algorithms complemented with classical data fusion techniques to compensate performance degradation due to sensor behaviour over time.

SENER

Álvaro Martínez
alvaro.martinez@aeroespacial.sener

Jesús Ramírez
jesus.ramirez@aeroespacial.sener

Francesco Cacciatore
francesco.Cacciatore@aeroespacial.sener

THANK YOU

www.aerospace.sener

www.linkedin.com/company/sener

www.youtube.com/user/senerengineering